

Evolution from localized to intermediate valence regime in $\text{Ce}_2\text{Cu}_{2-x}\text{Ni}_x\text{In}$

A P Pikul and D Kaczorowski

Institute of Low Temperature and Structure Research, Polish Academy of Sciences, P Nr 1410, 50-590 Wrocław 2, Poland

E-mail: A.Pikul@int.pan.wroc.pl

Abstract. Polycrystalline samples of the solid solution $\text{Ce}_2\text{Cu}_{2-x}\text{Ni}_x\text{In}$ were studied by means of x-ray powder diffraction, magnetic susceptibility and electrical resistivity measurements performed in a wide temperature range. Partial substitution of copper atoms by nickel atoms results in quasi-linear decrease of the lattice parameters and the unit cell volume of the system. The lattice compression leads to an increase in the exchange integral and yields a reversal in the order of the magnetic $4f^1$ and nonmagnetic $4f^0$ states, being in line with the Doniach phase diagram. In the localized regime, where an interplay of the Kondo scattering and the crystalline electric field effect takes place, the rise in the hybridization strength is accompanied with relative reduction in the scattering conduction electrons on excited crystal field levels.

PACS numbers: 75.20.Hr; 75.30.Mb; 72.15.Qm

Submitted to: *J. Phys.: Condens. Matter*

1. Introduction

Ternary intermetallics $\text{Ce}_2\text{Cu}_2\text{In}$ and $\text{Ce}_2\text{Ni}_2\text{In}$ crystallize in a primitive tetragonal structure of the Mo_2FeB_2 type (space group $P4/mbm$) with the lattice parameters $a = 7.7368(6)$ Å, $c = 3.9240(3)$ Å for the former phase, and $a = 7.5305(3)$ Å, $c = 3.7223(2)$ Å for the latter one [1]. The physical properties of $\text{Ce}_2\text{Cu}_2\text{In}$ indicate well localized magnetism due to the presence of stable Ce^{3+} ions. The compound orders antiferromagnetically at the Néel temperature $T_N = 5.5$ K, and its electrical resistivity is dominated by an interplay of strong Kondo and crystalline electric field interactions. In contrast, the $\text{Ce}_2\text{Ni}_2\text{In}$ compound exhibits features characteristic of intermediate valence systems, with partly delocalized $4f$ electrons of cerium [1, 2].

Since both compounds are isostructural, the qualitative difference in their ground states results exclusively from swapping copper atoms for nickel atoms. This fact motivated us to perform alloying studies of $\text{Ce}_2\text{Cu}_{2-x}\text{Ni}_x\text{In}$ as a unique opportunity to investigate an evolution of a $4f$ system from fully localized regime to well defined intermediate valence state, that is predicted by the Doniach diagram [3]. It is worth

noting that systematic studies of such evolution are often difficult (or even impossible) due to either relatively small difference between the ground states of two isostructural parent compounds or different crystal structures of the two terminal phases. In other words, such experimental studies usually cover only part of the Doniach diagram, e.g. quantum critical region.

In this paper we present the results of magnetic and electrical transport measurements of the solid solution $Ce_2Cu_{2-x}Ni_xIn$, performed in a wide temperature range, using polycrystalline samples. We demonstrate a prominent evolution of the main physical characteristics of the system upon increasing nickel content, and interpret the experimental data in terms of some theoretical models developed for localized and intermediate valence states. We argue, that the Cu/Ni substitution leads to an increase in the exchange integral, which yields a reversal in the order of the magnetic $4f1$ and nonmagnetic $4f0$ states. Moreover, the rise in the exchange integral brings about a diminishing influence of excited crystal field levels on the electrical transport in the system studied.

2. Experimental details

Polycrystalline samples of $Ce_2Cu_{2-x}Ni_xIn$ were prepared by arc melting stoichiometric amounts of the elemental components in titanium gettered argon atmosphere. The pellets were turned over and remelted several times to ensure good homogeneity. No further heat treatment was given to the as cast ingots.

Quality of the products was verified by X-ray powder diffraction (Stoe diffractometer with Cu $K\alpha_1$ radiation) and energy dispersive X-ray spectroscopy (Phillips 515 scanning electron microscope equipped with EDAX PV 9800 spectrometer). All the diffractograms were easily indexed within the expected primitive tetragonal structure. The microprobe analysis showed that the samples are nearly single phase (with minor traces of unidentified impurities) and their compositions are close to the nominal ones.

The magnetic properties were studied at temperatures 1.7 – 400 K and in magnetic fields up to 5 T using a commercial Quantum Design SQUID magnetometer. Electrical resistivity was measured on bar-shaped samples in zero field from 4.2 K up to room temperature, using a home-made setup.

3. Results and discussion

3.1. Crystal structure

Analysis of the X-ray diffraction patterns (not given here) confirmed that substitution of copper atoms by nickel atoms does not change the crystal structure of the system. It revealed also that the lattice parameters and the unit cell volume of the $Ce_2Cu_{2-x}Ni_xIn$ alloys systematically decrease (in a quasi-linear manner) with increasing nickel content from $a = 7.7368(6)$ Å, $c = 3.9240(3)$ Å and $V = 234.88$ Å³ for Ce_2Cu_2In to $a = 7.5305(3)$ Å, $c = 3.7223(2)$ Å and $V = 211.09$ Å³ for Ce_2Cu_2In [1] (see figure 1).

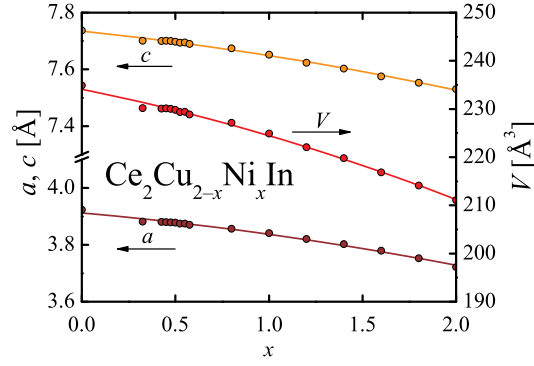


Figure 1. Lattice parameters a and c and unit cell volume V of selected alloys $\text{Ce}_2\text{Cu}_{2-x}\text{Ni}_x\text{In}$ as a function of the nominal nickel content x .

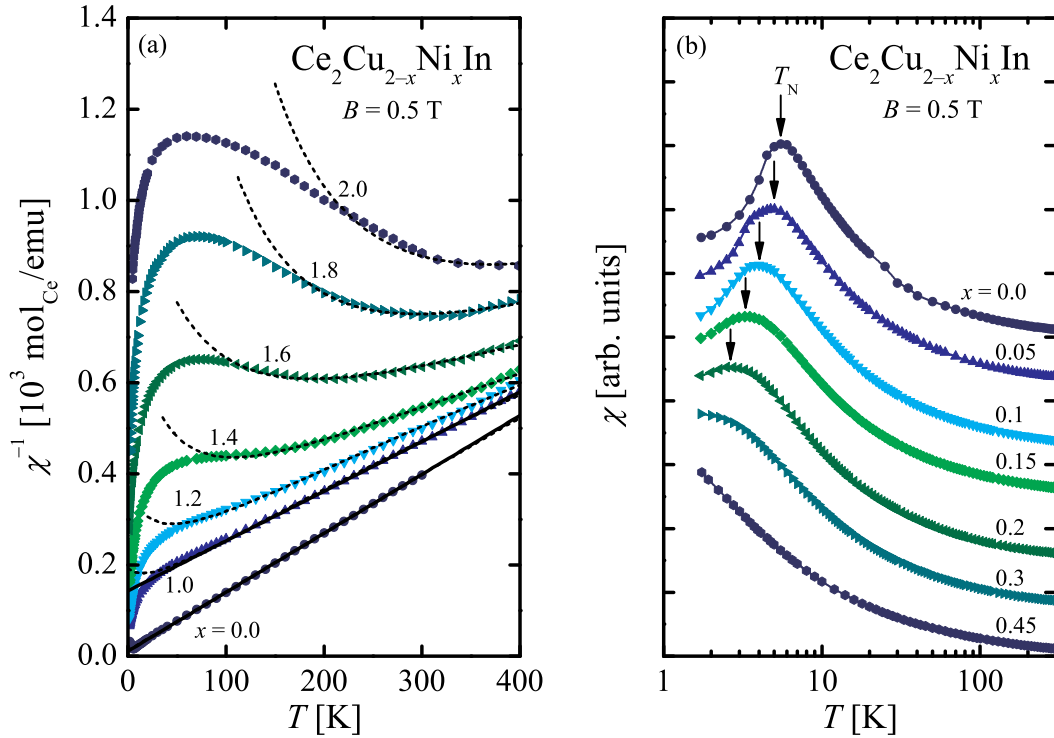


Figure 2. (a) Inverse magnetic susceptibility χ^{-1} of selected alloys $\text{Ce}_2\text{Cu}_{2-x}\text{Ni}_x\text{In}$ as a function of temperature T . Straight solid lines represent Curie-Weiss fittings; results for $0.00 < x < 1.00$ are omitted for the sake of clarity. (b) Magnetic susceptibility χ of $\text{Ce}_2\text{Cu}_{2-x}\text{Ni}_x\text{In}$ with $x \leq 0.45$ vs. T . Solid curves serve as guides for the eye and the arrows mark the Néel temperature T_N . x is the nominal composition.

3.2. Magnetic properties

Figure 2(a) presents the temperature dependencies of the inverse magnetic susceptibility of the alloys studied. As seen, $\chi^{-1}(T)$ measured for the Cu rich alloys (i.e. for $x \leq 1.00$) exhibit above about 100 K a linear behaviour given by the conventional Curie-Weiss

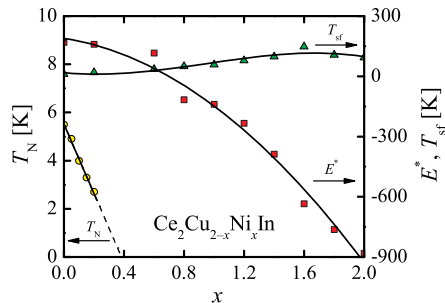


Figure 3. Néel temperature T_N , excitation energy E^* and spin fluctuation temperature T_{sf} of $Ce_2Cu_{2-x}Ni_xIn$ as a function of the nominal nickel content x . Solid and dashed lines serve as guides for the eye.

law:

$$\chi(T) = \frac{1}{8} \frac{\mu_{\text{eff}}^2}{T - \theta_p}, \quad (1)$$

where μ_{eff} is the effective magnetic moment and θ_p stands for the Weiss temperature. Least squares fittings of (1) to the experimental data collected for the alloys with $x \leq 1.00$ [see the solid lines in figure 2(a)] yielded nearly constant μ_{eff} of about 2.5–2.6 μ_B and θ_p decreasing monotonically from about -16 K for Ce_2Cu_2In (in agreement with [1]) to -51 K for $Ce_2Cu_{1.0}Ni_{1.0}In$. The obtained values of the effective magnetic moments are close to the theoretical one calculated for free Ce^{3+} ions (i.e. 2.54 μ_B) and point at the presence of well localized $4f$ electrons of cerium. The increase in the absolute value of the Weiss temperature can be ascribed to the enhancement of the hybridization strength between conduction electrons and $4f$ shells, expected for rising the Ni content.

The latter hypothesis is in line with further evolution of $\chi^{-1}(T)$, that is observed for the alloys with $x > 1$. Along with increasing the nickel content, the inverse magnetic susceptibility deviates more and more from the Curie–Weiss behaviour, suggesting progressive delocalization of the $4f$ electrons (i.e. evolution from the state $4f^1$ to the configuration $4f^0$).

According to the interconfiguration fluctuation (ICF) model developed by Sales and Wohleben [4], the magnetic susceptibility of the $4f$ electron compounds can be described as a sum of susceptibilities of two states: $4f^n$ and $4f^{n-1}$. Respectively, the states are characterized by well defined angular momenta J_n and J_{n-1} , the degeneracies $2J_n + 1$ and $2J_{n-1} + 1$, the Hund’s-rule effective magnetic moments μ_n and μ_{n-1} , and the energies E_n and E_{n-1} . The total magnetic susceptibility $\chi(T)$ of such a system can be expressed as:

$$\chi(T) = \frac{1}{8} \frac{\nu(T)\mu_n^2}{T + T_{sf}} + \frac{1}{8} \frac{[1 - \nu(T)]\mu_{n-1}^2}{T + T_{sf}}, \quad (2)$$

with the fractional occupation $\nu(T)$ of the $4f^n$ state:

$$\nu(T) = \frac{(2J_n + 1)}{(2J_n + 1) + (2J_{n-1} + 1) \exp[-E^*/(T + T_{sf})]}, \quad (3)$$

where T_{sf} is the spin-fluctuation temperature related to the transition rate ω_f between the two electron configurations involved ($k_B T_{sf} = \hbar\omega_f$), and E^* is the energy difference between the two $4f$ states ($E^* = E_{n-1} - E_n$), expressed in kelvins.

In cerium compounds, there are two possible configurations of the $4f$ shell: $4f^1$ (with $J_1 = \frac{5}{2}$ and $\mu_1 = 2.54 \mu_B$) and $4f^0$ (with $J_0 = 0$ and $\mu_0 = 0$). Hence, (2) and (3) take the form, respectively:

$$\chi(T) = \frac{1}{8} \frac{\nu(T)(2.54\mu_B)^2}{T + T_{sf}}, \quad (4)$$

and:

$$\nu(T) = \frac{6}{6 + \exp[-E^*/(T + T_{sf})]}, \quad (5)$$

with $E^* = E_0 - E_1$. According to this notation, in systems with the magnetic ground state $4f^1$ (e.g. magnetically ordered compounds, Kondo and heavy fermion systems) E^* is positive, while in the intermediate valence systems, in which the $4f^1$ configuration is the excited state, E^* is negative. For $E^* \geq 0$, the fractional occupation ν of the ground $4f^1$ state is weakly dependent on temperature and decreases from 1 (for $E^* \rightarrow +\infty$) to $6/7$ (for $E^* = 0$), and the associated magnetic moment changes from $2.54 \mu_B$ to $2.35 \mu_B$, respectively. Thus, the system exhibits features characteristic of localized magnetism, and (4) is a good approximation of the Curie–Weiss law. In turn, for $E^* < 0$, a characteristic maximum in $\chi(T)$ develops with increasing $|E^*|$, yet the Curie–Weiss behaviour can still be observed at high enough temperatures ($T \gg |E^*|$).

The magnetic susceptibility of the alloys $Ce_2Cu_{2-x}Ni_xIn$ seems to nicely follow the predictions of the ICF model. The experimental data can be described at elevated temperatures by (4) modified by adding a constant term χ_0 , which accounts for possible temperature independent paramagnetic and diamagnetic contributions to the total magnetic susceptibility (cf. [1, 5]), i.e.:

$$\chi(T) = \frac{1}{8} \frac{\nu(T)(2.54\mu_B)^2}{T + T_{sf}} + \chi_0. \quad (6)$$

Least squares fittings of (6) to the experimental data [see the dashed lines in figure 2(a) and figure 3] yielded E^* decreasing monotonically from $+169(18)$ K for Ce_2Cu_2In to $-882(9)$ K for Ce_2Ni_2In (in agreement with the value of -884 K, reported previously [1]). The parameter T_{sf} was found to increase from $+11(1)$ K to $93(4)$ K, respectively, in a non-linear manner with a local maximum of $147(5)$ K for $Ce_2Cu_{0.4}Ni_{1.6}In$. In turn, the temperature independent term was found to be nearly constant in the whole series of the alloys and equal to $\chi_0 \sim 10^{-4}$ emu/mol.

As apparent from figure 2(a), at low temperatures the experimental $\chi^{-1}(T)$ variations measured for strongly intermediate valent alloys significantly deviate from the predictions of the ICF model (note Curie-like tails $\chi \sim 1/T$). Such a behaviour is

often observed in the intermediate valence systems and can be ascribed to the presence of paramagnetic impurities (cf. [1]). While in the localized regime the latter contribution is negligible, in the intermediate valence state (exhibiting relatively weak magnetism) it becomes significant and thus strongly modifies the expected ICF curvature of $\chi^{-1}(T)$.

The change of E^* with increasing the nickel content (figure 3) is in line with the observed evolution of the magnetic properties of the system $Ce_2Cu_{1-x}Ni_xIn$. One should note however, that the ICF model does not take into account i.a. the crystal electric field effect and magnetic correlations, which are also expected to play some role in the alloys studied (cf. [1]). Therefore, the derived absolute values of E^* can differ from the actual energy difference between the $4f^1$ and $4f^0$ configurations, especially in the localized regime.

Figure 2(b) displays the temperature dependencies of the magnetic susceptibility $\chi(T)$ for the alloys with $x \leq 0.45$, which exhibit well localized magnetic moments. Clearly, the compound Ce_2Cu_2In orders antiferromagnetically at the Néel temperature $T_N = 5.5$ K, in agreement with the previous finding [1]. With increasing x , T_N [defined as a maximum on the $\chi(T)$ curve] rapidly decreases. For $x = 0.45$, hardly any anomaly is visible in $\chi(T)$, at least in the temperature range studied. Extrapolation of the dependence $T_N(x)$ to the absolute zero temperature (see the dashed line in figure 3) yields the critical concentration x_c of about 0.4. In parallel with the suppression of T_N , one observes gradual broadening of the maximum in $\chi(T)$ that manifests the antiferromagnetic phase transition. This finding suggests that the quantum critical phase transition smears out and hence no quantum critical state could be reached, as concluded also e.g. in $CePd_{1-x}Rh_x$ [6, 7, 8].

3.3. Electric properties

The temperature variations of the electrical resistivity of $Ce_2Cu_{1-x}Ni_xIn$ and the nonmagnetic reference La_2Cu_2In (normalized to room temperature values) are presented in figure 4. While the $\rho(T)$ curve obtained for the La sample is characteristic of simple metals, the resistivity of the parent compound Ce_2Cu_2In exhibits features of a magnetically ordered dense Kondo system. In the paramagnetic region, $\rho(T)$ forms a broad hump at about 100 K and exhibits a negative logarithmic slope below about 20 K, both manifesting the Kondo scattering of conduction electrons on crystalline electric field $4f$ sublevels (cf. [1]). A drop of the resistivity at about 6 K results from the antiferromagnetic phase transition. For the alloys with $x > 0$, the magnetic phase transition could not be evidenced because of the temperature limit of our resistivity measurements (≈ 4 K). With increasing the nickel content, the low temperature $-\log T$ contribution becomes dominant and for $x = 0.4$ it entirely merges with the hump at elevated temperatures. Over an extended temperature range $\rho(T)$ of this alloy exhibits a single nearly logarithmic slope [figure 4(a)]. For higher x , the low temperature resistivity evolves into a T^2 dependence [see dashed curve in figure 4(b)], that signals the intermediate valence behaviour.

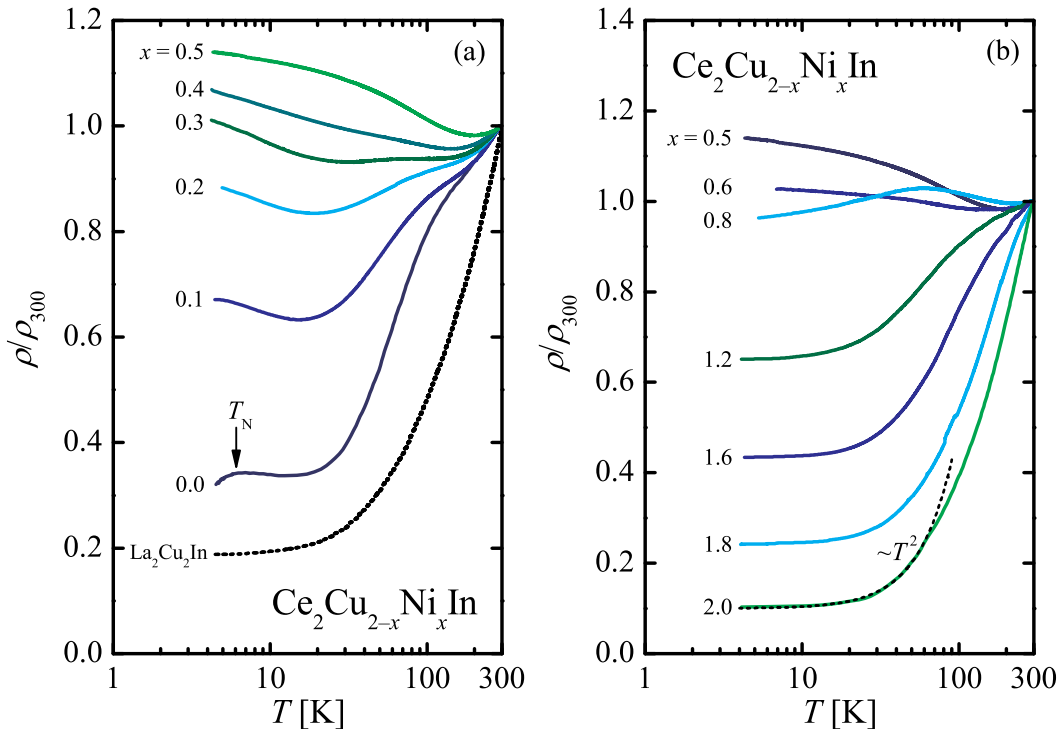


Figure 4. Electrical resistivity ρ of $\text{Ce}_2\text{Cu}_{2-x}\text{Ni}_x\text{In}$ and its non-magnetic reference $\text{La}_2\text{Cu}_2\text{In}$, normalized per room temperature value ρ_{300} , as a function of temperature T . x is the nominal composition and the arrow marks the Néel temperature T_N . The data for $\text{La}_2\text{Cu}_2\text{In}$ are taken from [1].

In order to shed more light on the observed evolution of $\rho(T)$ of the alloys $\text{Ce}_2\text{Cu}_{1-x}\text{Ni}_x\text{In}$ with $x \leq 0.4$, we derived the magnetic contribution ρ_{mag} to their total resistivity by subtracting the phonon contribution to $\rho(T)$ of $\text{La}_2\text{Cu}_2\text{In}$ (cf. [1]). The $\rho_{\text{mag}}(T)$ curve obtained for $\text{Ce}_2\text{Cu}_2\text{In}$ revealed that the hump in $\rho(T)$ results from the presence of a distinct maximum in ρ_{mag} followed by another $-\log T$ dependence at high temperatures [figure 5(a)]. Moreover, two logarithmic slopes are visible also in the other Cu-rich alloys, in which the maximum at 100 K is somewhat obscured by the low temperature $-\log T$ dependence.

According to the Cornut–Coqblin model [9], in the localized regime with the magnetic ground state the interplay of the Kondo effect and the crystalline electric field (CEF) results in the magnetic contribution to the total resistivity, which can be expressed as:

$$\rho_i(T) = aJ_{\text{ex}}^2 \frac{\lambda_i^2 - 1}{\lambda_i(2J_1 + 1)} + 2aN(E_F)J_{\text{ex}}^3 \frac{\lambda_i^2 - 1}{(2J_1 + 1)} \log \frac{T}{D_i}, \quad (7)$$

where $J_1 = 5/2$, λ_i denotes the effective degeneracy of the $4f^1$ state, J_{ex} is the negative exchange integral, $N(E_F)$ is the density of states at the Fermi level, D_i is the effective cutoff parameter, and a is a constant. In the case of Ce^{3+} ions experiencing a tetragonal crystal electric field potential, the sixfold degenerated $4f^1$ multiplet splits into three doublets located at the energies $\Delta_1 \equiv 0 < \Delta_2 < \Delta_3$. Population of these levels depends

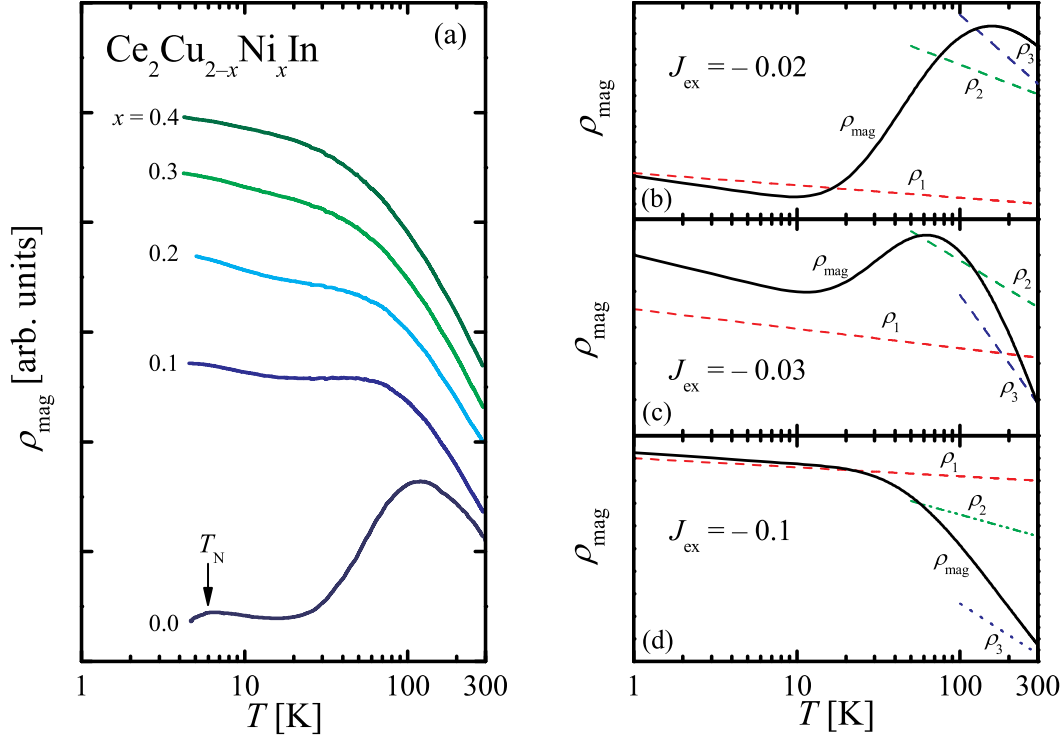


Figure 5. (a) Temperature dependencies of a Kondo contribution ρ_{mag} to the electrical resistivity of $Ce_2Cu_{2-x}Ni_xIn$. Panels (b), (c), and (d) display theoretical $\rho_{\text{mag}}(T)$ of a Ce^{3+} -based system and tetragonal CEF potential [equation (8)], calculated for different values of J_{ex} . The assumed CEF splitting scheme: $\Delta_1 = 0$ K, $\Delta_2 = 50$ K and $\Delta_3 = 100$ K. The dashed lines represent the individual ρ_i contributions [equation (7)] for fully populated crystal field levels.

on the temperature, so the effective degeneracy of the $4f^1$ state increases with increasing T from $\lambda_1 = 2$ (ground doublet) at absolute zero temperature, to $\lambda_2 = 4$ (pseudoquartet) at elevated T , to $\lambda_3 = 6$ (pseudosextet) at high temperatures. From (7) it becomes clear that the slope and the magnitude of $\rho_i(T)$ depend on λ_i , so for well separated doublets one can observe up to three $-\log T$ slopes in the magnetic contribution to the resistivity.

However, from the point of view of the present study, it is more important to note that the relative magnitudes of the particular $\rho_i(T)$ contributions [equation (7)] may vary also with J_{ex} , making the observation of the separated Kondo slopes difficult (cf. [9]). Assuming Boltzman-like thermal excitations of the crystalline electric field doublets (in line with the Cornut–Coqblin approach [9]), the Kondo contribution ρ_{mag} to the electrical resistivity can be expressed as:

$$\rho_{\text{mag}}(T) = \rho_1 + (\rho_2 - \rho_1) \exp\left(-\frac{\Delta_2}{T}\right) + (\rho_3 - \rho_2) \exp\left(-\frac{\Delta_3}{T}\right). \quad (8)$$

Note, that the contributions ρ_2 and ρ_3 include already ρ_1 and ρ_2 , respectively. In order to avoid their multiplication, two corrections, i.e. $-\rho_1 \exp(-\Delta_2/T)$ and $-\rho_2 \exp(-\Delta_3/T)$, were added. In order to check the influence of magnetic exchange on the overall character of $\rho_{\text{mag}}(T)$, we made a few simulations using a fixed crystal electric field scheme (2:2:2

with $\Delta_1 = 0$ K, $\Delta_2 = 50$ K, and $\Delta_3 = 100$ K) and varying the arbitrary chosen value of J_{ex} . For simplicity, the constants a , $N(E_F)$, and D_i were assumed to be independent of J_{ex} and equal to 1. Figure 8(b), figure 8(c) and figure 8(d) display the results of these calculations.

As shown in figure 8(b), for low absolute values of J_{ex} the magnitude of the ground doublet contribution ρ_1 is much less than the pseudo-quartet (ρ_2) and pseudo-sextet (ρ_3) contributions. As a consequence, the crossover between the crystal field levels manifests itself as a distinct maximum in $\rho_{\text{mag}}(T)$. Upon increasing $|J_{\text{ex}}|$, ρ_1 increases and becomes of the same order of magnitude as ρ_2 and ρ_3 , and the maximum in $\rho_{\text{mag}}(T)$ becomes less pronounced [figure 5(c)]. Finally, for large $|J_{\text{ex}}|$, the magnitude of ρ_1 is higher than ρ_2 and ρ_3 , so the crossover between the logarithmic slopes in $\rho_{\text{mag}}(T)$ is monotonic [figure 5(d)].

Although any quantitative analysis of the resistivity data in terms of (8) is hampered by polycrystalline nature of the specimens studied (effects of magnetocrystalline anisotropy, inter-grains resistance, possible internal cracks, etc.), it is worth emphasizing the qualitative similarity of the experimental [figure 5(a)] and model curves [figure 5(b), figure 5(c) and figure 5(d)]. Their evolution with increasing the Ni content can thus be attributed to the increase in the strength of the hybridization, as it has been done for the magnetic susceptibility data.

4. Summary and conclusions

The partial substitution of Cu by Ni in the antiferromagnetically ordered compound Ce_2Cu_2In results in a monotonic compression of its unit cell (up to 10%), accompanied by a drastic change of the physical properties of the system. In particular, the magnetic measurements of $Ce_2Cu_{2-x}Ni_xIn$ revealed continuous evolution from the localised magnetic moments regime for $x \lesssim 0.6$ to the fluctuating valence state for $x \gtrsim 1.6$. The detailed analysis of the inverse magnetic susceptibility data within the ICF model yielded reversal of the order of the magnetic $4f^1$ and nonmagnetic $4f^0$ levels in the alloys with $0.6 \lesssim x \lesssim 1.6$. In other words, the $4f^1$ level, being the ground state in the Cu-rich alloys and lying *below* the Fermi level (equivalent to the $4f^0$ configuration), becomes an excited state in the Ni-rich alloys, lying *above* the Fermi level.

Deeply in the localized regime, the Ce magnetic moments order antiferromagnetically, and the Néel temperature decreases quasi-linearly with increasing the nickel content from 5.5 K in Ce_2Cu_2In down to 2.7 K in $Ce_2Cu_{1.2}Ni_{0.8}In$. Simultaneous significant broadening of the maximum in $\chi(T)$ at T_N indicates possible smearing of the phase transition at temperatures approaching the absolute zero. The analysis of the temperature dependencies of the electrical resistivity of the $Ce_2Cu_{2-x}Ni_xIn$ series revealed an evolution of the system from the dense Kondo lattice regime towards the nonmagnetic metal regime, controlled mainly by the increase in the exchange integral.

All the presented findings are in line with the Doniach picture of Kondo systems, which predicts a change in the character of the ground state from long range magnetic

order to intermediate valence. This transformation is induced by an increase in the value of the exchange integral J_{ex} that measures the hybridization strength. For $Ce_2Cu_{2-x}Ni_xIn$, the increase of J_{ex} with increasing x is likely a consequence of the observed compression of the unit cell volume. Simultaneous reduction in a number of the $3d$ electrons, which could probably lead to some decrease in J_{ex} , seems to have less significant influence on the physical properties of the system. To verify our hypothesis detailed spectroscopic studies of the $Ce_2Cu_{2-x}Ni_xIn$ series are indispensable.

Acknowledgments

This work was supported by the Polish Ministry of Science and Higher Education within research grant no. N N202 102338.

References

- [1] Kaczorowski D, Rogl P and Hiebl K 1996 *Phys. Rev.* **B 54** 9891
- [2] Hauser H, Michor H, Bauer E, Hilscher G and Kaczorowski D 1997 *Physica* **B 230–232** 211
- [3] Doniach S 1977 *Valence Instabilities and Related Narrow Band Phenomena* ed Parks R D (New York: Plenum Press) p 169
- [4] Sales B B and Wohlleben D K 1975 *Phys. Rev. Lett.* **18** 1240
- [5] Pecharsky V K, Gschneidner J K A and Müller L L 1991 *Phys. Rev.* **B 43** 10906
- [6] Sereni J G, Westerkamp T, KÜchler R, Caroca-Canales N, Gegenwart P and Geibel C 2007 *Phys. Rev.* **B 75** 024432
- [7] Pikul A P, Caroca-Canales N, Deppe M, Gegenwart P, Sereni J G, Geibel C and Steglich F 2006 *J. Phys.: Condens. Matter* **18** L535
- [8] Westerkamp T, Deppe M, KÜchler R, Brando M, Geibel C, Gegenwart P, Pikul A P and Steglich F 2009 *Phys. Rev. Lett.* **102** 206404
- [9] Cornut D and Coqblin B 1972 *Phys. Rev.* **B 5** 4541